

Wavelength dependent studies of nonlinear absorption in zinc *meso*-tetra(*p*-methoxyphenyl)tetrabenzoporphyrin (Znmp TBP) using Z-scan technique

N. K. M. NAGA SRINIVAS,¹ S. VENUGOPAL RAO,^{1†} D. V. G. L. N. RAO,² B. K. KIMBALL,³ M. NAKASHIMA,³ B. S. DECRISTOFANO³ and D. NARAYANA RAO^{1*}

¹School of Physics, University of Hyderabad, Hyderabad 500 046, India

²Department of Physics, University of Massachusetts, Boston, MA 02125, USA

³US Army Research Development and Engineering Center, Natick, MA 01760, USA

Received 11 December 2000

Accepted 15 December 2000

ABSTRACT: We report here, our experimental results and theoretical analysis of the dispersion data of nonlinear absorption in zinc *meso*-tetra(*p*-methoxyphenyl)tetrabenzoporphyrin (ZnmpTBP). Using a ns optical parametric oscillator (OPO) we obtain the open aperture Z-scan data over the visible region starting from 480 nm to 600 nm. We use a more general five-level model for evaluating the excited state parameters like excited state absorption coefficients, two-photon absorption coefficient, etc. Due to its large excited state absorption cross-sections this material acts as a very good candidate for a broadband optical limiter in the visible region. Copyright © 2001 John Wiley & Sons, Ltd.

KEYWORDS: Z-scan technique; porphyrins; excited state absorption; two-photon absorption; optical limiting

INTRODUCTION

With the advent of high power ps and fs lasers the necessity for protection of the sensors and the eye from intense laser fields has increased enormously over the last few years. Various mechanisms have been proposed for optical limiting which include scattering 1, thermal/nonlinear refractive beam spreading 2, excited state absorption (ESA)/reverse saturable absorption (RSA) 3, two-photon absorption/multi-photon absorption (TPA) 4, photorefractive 5, free carrier absorption in semiconductors 6, polarization changes 7, 8, etc. Different materials investigated, in the solid and liquid forms, are fullerenes 9, porphyrins/metalloporphyrins 10, phthalocyanines 11, inorganic clusters 12, organometallics 13, organic dyes 14, particle suspensions 15, liquid crystals 16, bacteriorhodopsin 17, photonic band gap materials 18, christiansen filter 19, nanosols 20, and chinese tea 21. Several reviews have been published on mechanisms for optical limiting, material requirement, optimization and realization 22–25. The minimum criteria identified for a material to act as an effective optical limiter are: (1) low limiting threshold and large dynamic range (over a wide range of input fluences); (2) longer excited state lifetime to accumulate the popula-

tion; (3) high optical damage threshold; (4) broadband response; (5) fast response time; and (6) high linear transmittance, optical clarity, and robustness. Among the above-mentioned materials fullerenes, porphyrins, and phthalocyanines have been found to satisfy the majority of the criteria with a few exceptions, e.g. the damage threshold. Since the mechanism of limiting in these materials depends on absorption of excited molecules it is important to characterize the excited state dynamics and evaluate

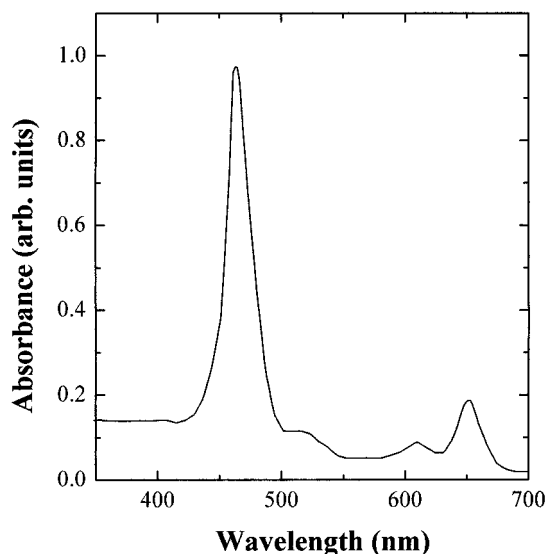


Fig. 1. Absorption spectrum of the sample (in THF).

Andrews, St Andrews, Scotland KY16 9SS, UK.

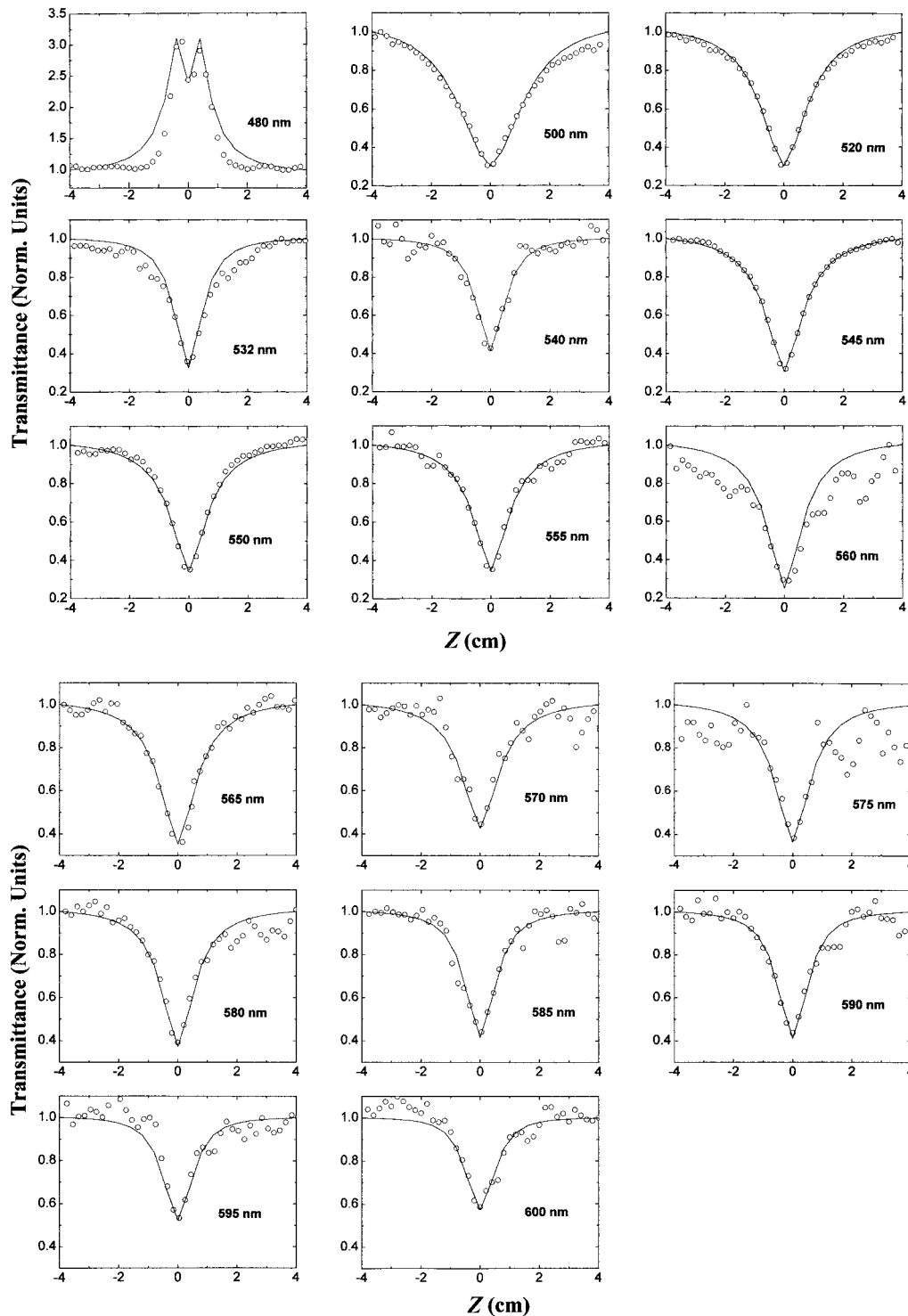


Fig. 2. Open aperture Z-scan data (scattered points) and the theoretical fits (solid lines) obtained using the five-level model for wavelengths ranging from 480 nm to 600 nm.

parameters like absorption cross-sections, lifetimes, etc. to optimize them in the making of a realistic device. A recent paper, where a RSA material (a phthalocyanine) is used along with CS_2 , reports a high figure of merit (defined as the ratio of linear transmittance to minimum transmittance at high energy) within the measured dynamic range of the limiter, as ~ 7500 , the largest reported to date 26. With such a goal in mind we attempted a comparative study of C_{60} , Zinc *meso*-tetra-(*p*-methoxyphenyl)tetrabenzoporphyrin

(ZnmpTBP), and a copper phthalocyanine (CuPC) for optical limiting over a broad spectrum (440 nm to 680 nm) using the Z-scan technique 27.

Here, we report on the dispersion studies of nonlinear absorption in a tetrabenzoporphyrin (ZnmpTBP). RSA and optical limiting in porphyrins are well-established concepts 28, 29. However, most of the earlier studies are at a single wavelength. For fs and ps pulse excitation, triplet level contribution to the nonlinear absorption can be neglected

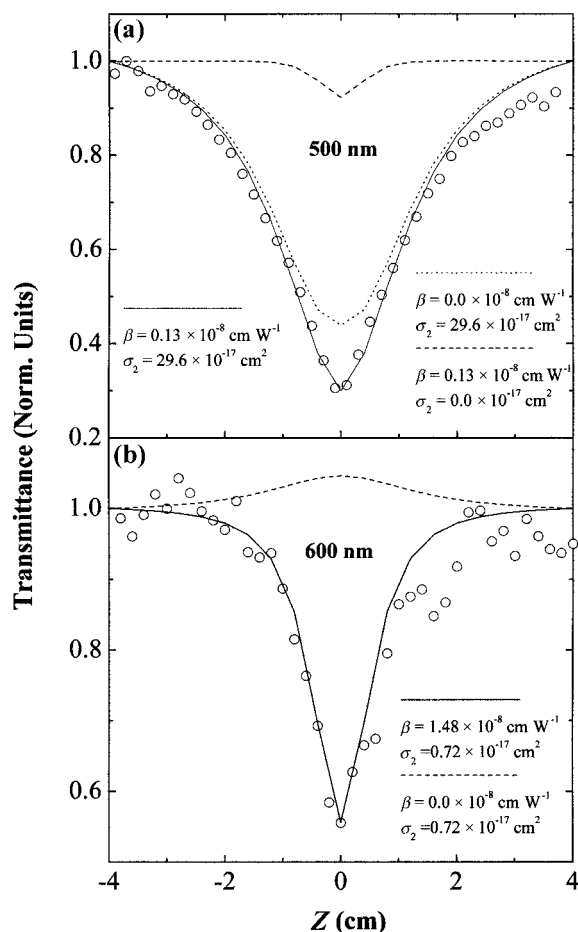


Fig. 3. Effect of β and σ_2 on the open aperture Z-scan curves at (a) 500 nm and (b) 600 nm.

due to the slower intersystem crossing rate whereas with ns pulses the triplet levels do play an important role. Depending on the pump intensity, temporal duration and wavelength, absorption could be: (1) from the ground state S_0 to the first excited singlet state S_1 and then to the T_1 state through inter-system crossing; (2) directly from S_0 to S_n states (two-photon absorption); (3) from the first excited singlet state S_1 to higher excited states S_n (ESA/RSA); or (4) from T_1 to T_n states (ESA/RSA). We consider here, a more general five-level model and fit our open aperture Z-scan data to the above model, while incorporating all the above nonlinear absorption mechanisms.

EXPERIMENT

We employed a commercial optical parametric oscillator (OPO) (MOPO, laser by Spectra Physics) pumped by the third harmonic (355 nm) of a Quanta Ray Nd:YAG laser with a repetition rate of 10 Hz and tunable in the range of 380–1000 nm. The pulse duration of the laser was 6 ns and an aperture of 1.4 mm was used at the output of the MOPO laser to obtain a smooth profile in the far field. The energy after the aperture was varied from 0.2 mJ/pulse to 2 mJ/pulse depending on the wavelength. The input beam was focused using a lens of focal length ~ 50 mm into a 1-mm quartz cell containing the sample dissolved in spectroscopic grade tetrahydrofuran (THF). The input energy was

monitored using a fast photo-diode and the output was measured using a similar photo-diode. ZnmpTBP (>99% pure) solutions with concentration in the range $\sim 10^{-4}$ – 10^{-3} M were freshly prepared and used for the study. Open aperture Z-scans were obtained in the wavelength region covering 480 nm to 600 nm. The values of beam waist at focus were ~ 20 – 30 μm and the corresponding peak intensities were $\sim 10^8$ to 10^9 W cm^{-2} . The Rayleigh ranges were calculated to be ~ 3 mm to 6 mm depending on the wavelength. Rate equations for the five-level model (S_0 , S_1 , S_n , T_1 , and T_n states) are:

$$\frac{dN_0}{dt} = -\frac{\sigma_0 I N_0}{\hbar\omega} - \frac{\beta I^2}{2\hbar\omega} + \frac{N_1}{\tau_1} + \frac{N_3}{\tau_4} \quad (1)$$

$$\frac{dN_1}{dt} = -\frac{\sigma_1 I N_1}{\hbar\omega} + \frac{\sigma_0 I N_0}{\hbar\omega} - \frac{N_1}{\tau_1} - \frac{N_1}{\tau_{\text{ISC}}} + \frac{N_2}{\tau_2} \quad (2)$$

$$\frac{dN_2}{dt} = \frac{\sigma_1 I N_1}{\hbar\omega} + \frac{\beta I^2}{2\hbar\omega} - \frac{N_2}{\tau_2} \quad (3)$$

$$\frac{dN_3}{dt} = -\frac{\sigma_2 I N_3}{\hbar\omega} - \frac{N_3}{\tau_4} + \frac{N_1}{\tau_{\text{ISC}}} + \frac{N_4}{\tau_3} \quad (4)$$

$$\frac{dN_4}{dt} = \frac{\sigma_2 I N_3}{\hbar\omega} - \frac{N_4}{\tau_3} \quad (5)$$

and the intensity transmitted through the sample is given by:

$$\frac{dI}{dz} = -\sigma_0 I N_0 - \sigma_1 I N_1 - \sigma_2 I N_3 - \beta I^2 \quad (6)$$

with:

$$I = I_{00} \times \left(\frac{\omega_0^2}{\omega^2(z)} \right) \times \exp\left(-\frac{t^2}{\tau_p^2}\right) \times \exp\left(-\frac{2 \times r^2}{\omega^2(z)}\right) \quad (7)$$

and:

$$\omega(z) = \omega_0 \left[1 + \left(\frac{z}{z_0} \right)^2 \right]^{1/2}; z_0 = \frac{\pi \times \omega_0^2}{\lambda}$$

where σ_0 is the ground state absorption cross-section, σ_1 and σ_2 are the excited state absorption cross-sections from S_1 and T_1 states, respectively, N_i 's are the corresponding populations in the different states, τ_i 's are the lifetimes of the excited states, z_0 is the Rayleigh range, ω_0 is the beam waist at focus, I is intensity as a function of r , t , and z , I_{00} is peak intensity at the focus of the gaussian beam, τ_p is the input pulse width used, β is the two-photon absorption cross-section, and τ_{ISC} is the intersystem crossing rate. The differential equations are solved numerically using the Runge–Kutta fourth-order method. The differential equations are first de-coupled and then integrated over time, length, and along the radial direction. Assuming the input beam to be a Gaussian, the limits of integration for r , t , and z are varied from 0 to ∞ , $-\infty$ to ∞ , and 0 to L (length of the sample), respectively. Typical number of slices used for r , t , and z are 60, 30, and 5, respectively. σ_1 , σ_2 , and β are then estimated through a least square fit of the experimental data.

RESULTS AND DISCUSSION

Figure 1 shows the UV-vis absorption spectrum of the

Table 1. Calculated values of different excited state parameters using a five-level model and comparison with those reported in the literature

σ_0 (10^{-17} cm ²)	σ_1 (10^{-17} cm ²)	σ_2 (10^{-17} cm ²)	$\beta \times 10^{-8}$ (cm W ⁻¹)	Ref.
				Our study
0.298	1.00	0.1	0.18	480 nm
1.478	3.00	29.6	0.13	500 nm
0.826	1.00	33.4	0.25	510 nm
0.739	1.00	27.5	0.27	520 nm
0.739	3.00	11.9	0.57	532 nm
0.910	3.00	11.0	0.60	540 nm
0.956	3.00	10.8	0.61	545 nm
1.000	3.00	10.7	0.60	550 nm
1.043	3.00	10.7	0.70	555 nm
1.000	6.00	10.5	0.70	560 nm
1.130	6.00	10.3	0.77	565 nm
1.261	6.00	9.00	0.82	570 nm
1.478	6.00	8.50	1.26	575 nm
1.696	6.00	4.90	1.28	580 nm
1.867	6.00	0.93	1.28	585 nm
2.130	6.00	0.78	1.30	590 nm
2.610	6.00	0.72	1.45	595 nm
3.174	6.00	0.72	1.48	600 nm
–	1.7	7.2	–	Chen <i>et al.</i> 28 ZnTPP 532 nm (35 ps)
σ_g		σ^a	(β_{eff})	Henari <i>et al.</i> 33 ZnTaP
0.35	–	1.2	1.48	532 nm (35 ps)
19.0		2.5	0.64	450 nm (500 ps)
		σ^a	(β_{eff})	Mishra <i>et al.</i> 28 ZnTPP
2.7	–	10.8	–	527 nm (20 ns)
				Guha <i>et al.</i> 10 ZnmpTBP
2.4 cm ^{-1b}	–	3.0 ± 0.25	2.5 ± 0.2	21 ps and 6 ns, 532 nm ZnmpTBP
3.8 cm ^{-1b}	–	3.0 ± 0.25	≤ 0.5	532 nm

^a Effective excited state cross-section.^b Linear absorbance.

sample recorded by a Shimadzu UV-160 A. The absorption spectrum of the ZnmpTBP sample matches very well with that reported in the literature 31. The Q-band is centered around 460 nm and the B-bands are around 610 nm and 650 nm. Figure 2 shows the open aperture Z-scan data (scattered points) and the theoretical fits (solid lines) obtained using the five-level model for wavelengths ranging from 480 nm to 600 nm. The ground state absorption cross-sections for different wavelengths are calculated using $\sigma_0 = \alpha/N$, where α is the linear absorption and N is the density of molecules per cm³. Depending on the wavelength, I_{00} is taken as $\sim 10^8$ – 10^9 W cm⁻², $\omega_0 \sim 20$ – 30 μ m, and $z_0 \sim 3$ – 6 mm. The relaxation time of the first excited state τ_{S1} , intersystem crossing time τ_{ISC} , and the lifetime of the first excited triplet state τ_{T1} are taken as 40 ps, 2 ns, and 200 μ s,

respectively. Our earlier studies, performed using degenerate four-wave mixing (DFWM) with incoherent light, indicate an excited state lifetime of ~ 40 ps for the S₁ 32. The relaxation times of the S_n and T_n states are taken as 100 fs. Excitation wavelengths are indicated for each Z-scan curve.

Figure 3 shows the effect of σ_2 and β at both 500 nm and 600 nm. Fig. 3(a) shows theoretical curves generated at 500 nm. The dotted line represents the curve with $\sigma_2 = 29.6 \times 10^{-17}$ cm² and $\beta = 0.0$ cm W⁻¹, whereas the solid line is generated with $\sigma_2 = 29.6 \times 10^{-17}$ cm² and $\beta = 0.13 \times 10^{-8}$ cm W⁻¹. We have also generated a dashed curve with $\sigma_2 = 0.0 \times 10^{-17}$ cm² and $\beta = 0.13 \times 10^{-8}$ cm W⁻¹ to show the contribution of σ_2 at this wavelength. All these curves are generated without varying other parameters ($\sigma_0 = 1.478 \times 10^{-17}$ cm², $\sigma_1 = 3.00 \times 10^{-17}$ cm²). Figure

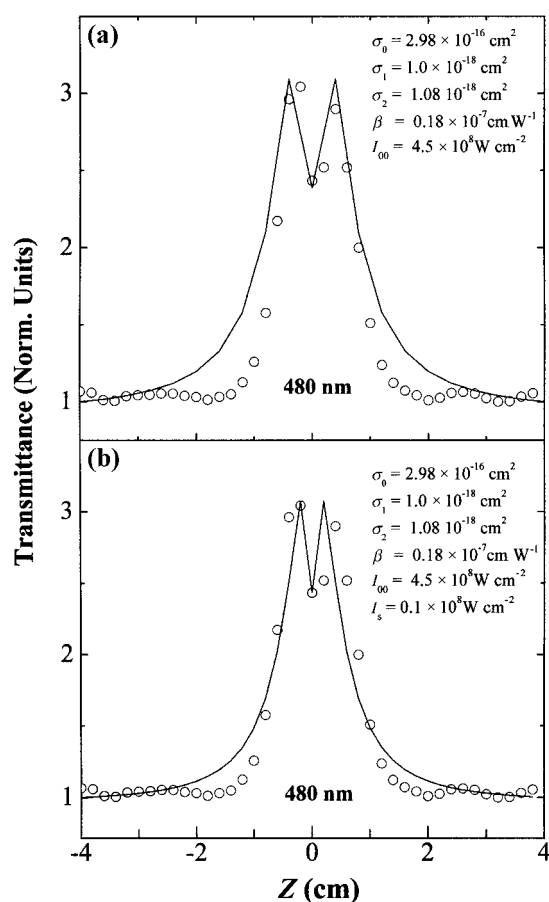


Fig. 4. Experimental (open circles) and theoretical open aperture Z-scan curves (solid lines) at 480 nm.

3(b) shows theoretical curves generated at 600 nm for $\sigma_0 = 3.174 \times 10^{-17} \text{ cm}^2$, $\sigma_1 = 6.00 \times 10^{-17} \text{ cm}^2$, $\sigma_2 = 0.72 \times 10^{-17} \text{ cm}^2$, $\beta = 0.0 \text{ cm W}^{-1}$ (dashed line) and $\beta = 1.48 \times 10^{-8} \text{ cm W}^{-1}$ (solid line) while keeping all other parameters the same. We can clearly see from Fig. 3(a) that variation in σ_2 shows significant effect on the curve at 500 nm. At 500 nm, σ_2 domination is evident as without σ_2 , the half width as well as the absorption at the focus (dotted lines in Fig. 3(a)) become too shallow compared to the experimental values. Therefore, at shorter wavelengths, both σ and β contribute to RSA behavior. Variation with β is found to be much more dramatic at 600 nm compared to the variation with σ_2 , indicating a dominance of β at longer wavelengths. Energy localization is dominant at this wavelength leading to a two-photon absorption process. Since the pulses used are of ns duration the intersystem crossing rate being 2 ns duration, and the lifetime of the triplet state is very high compared to the singlet, a variation in σ_1 has very little effect on the shape of the curves generated at 500 nm and 600 nm. Table 1 summarizes the σ_1 , σ_2 , and β values obtained from our measurements along with those reported in the literature for similar compounds.

In the wavelength region close to absorption peaks an increase in transmission with increased intensity was observed (SA). This is evident in the Z-scan curves at 480 nm, where there is an absorption band. Henari *et al.* 33 reported saturation of absorption at 450 nm with a similar porphyrin, again the excitation wavelength having

strong absorption, supporting our arguments. At these wavelengths the absorption from the ground state dominates in comparison to the excited state absorption coefficient.

In order to see the effects of linear absorption and the saturation effect, we generated the curves shown in Fig. 4 with and without saturation of the first excited state S_1 . Figure 4(a) shows the curve (solid line) generated with linear absorption for $\sigma_0 = 2.98 \times 10^{-16} \text{ cm}^2$, $\sigma_1 = 1.0 \times 10^{-17} \text{ cm}^2$, $\sigma_2 = 1.08 \times 10^{-18} \text{ cm}^2$, and $\beta = 0.18 \times 10^{-7} \text{ cm W}^{-1}$ along with the experimental data (circles). Figure 4(b) shows the curve generated (solid line) saturation intensity $I_s = 0.1 \times 10^8 \text{ W cm}^{-2}$, with α_0 being replaced by $\alpha_0/(1 + I/I_s)$ 34. We observe better fit for the experimental data taking saturation effects for the S_1 level. This is understandable as the input intensities exceed that of the linear absorption. These large intensities lead to RSA behavior at the focal point with $\sigma_1 = 1.0 \times 10^{-17} \text{ cm}^2$, $\sigma_2 = 1.08 \times 10^{-18} \text{ cm}^2$, and $\beta = 0.18 \times 10^{-7} \text{ cm W}^{-1}$. Previous reports 35, 36 suggest saturation of the higher singlet states where they observe RSA and SA around the focal region (quite the opposite is observed here). In our studies we have employed a ns laser where the intensities cannot saturate the higher excited S_n states. At lower intensities all the population could get trapped in the first excited triplet states (T_1) thereby saturating the absorption. With still higher intensities the population is excited into the higher excited states (T_n) thereby giving rise to the small amount of RSA. Since the lifetime of the S_1 state is very small we do not expect saturation in that state.

Thus porphyrins show RSA behavior even around 480 nm at higher intensities, which has not been reported earlier. Porphyrins can therefore be used as RSA material over a much wider wavelength region than the transmission window (500–600 nm). The added advantage of porphyrins over other materials is that they can be cast into thin films by doping them in a suitable host (polymer, sol-gel, or glass) 29, 37. From these studies the strong contribution of the σ_2 is evident over the entire visible region studied. Efforts are being made to reduce the inter-system crossing rate thereby enhancing the role of triplets for RSA.

CONCLUSIONS

In conclusion we have studied the dispersion of nonlinear absorption in ZnmpTBP using open aperture Z-scan data obtained with an OPO. We evaluated the excited state absorption coefficients (σ_1 and σ_2) and two-photon absorption coefficient (β) using a five-level model. Our results indicate that TPA dominates at longer wavelength and ESA dominates at shorter wavelengths. When the excitation is into the absorption band we see saturation type of behavior. At higher intensities we observe RSA behavior even at these wavelengths. With strong RSA shown over a wide region ZnmpTBP is an attractive broadband optical limiter.

Acknowledgements

D. N. Rao acknowledges financial support from the Department of Science and Technology, India and thanks Professor Sukant Tripathy of Lowell, MA for the OPO facility.

REFERENCES

- Mansour K, Soileau MJ, Vanstryland EW. *J. Opt. Soc. Am.* 1992; **B9**: 1100.
- (a) Justus BL, Campillo AJ, Huston AL. *Opt. Lett.* 1994; **19**: 693; (b) Leite RC, Porto SPS, Damien TC. *Appl. Phys. Lett.* 1967; **10**: 100.
- Tutt LW, Kost A. *Nature* 1992; **356**: 225.
- (a) He GS, Gvishi R, Prasad PN, Reinhardt BA. *Opt. Commun.* 1995; **117**: 133; (b) He GS, Bhawalkar JD, Zhao CF, Prasad PN. *Appl. Phys. Lett.* 1995; **67**: 2433; (c) He GS, Xu GC, Prasad PN, Reinhardt BA, Bhatt JC, Dillard AG. *Opt. Lett.* 1995; **20**: 435.
- (a) Feinberg J. *J. Opt. Soc. Am.* 1982; **72**: 46; (b) Golomb MC, Yariv A. *J. Appl. Phys.* 1985; **57**: 4906.
- (a) Bogges TF, Smirl AL, Moss SC, Boyd IW, Stryland EWV. *IEEE J. Quantum Electron.* 1985; **21**: 488; (b) Sheik-Bahae M, Mukherjee P, Kwok HS. *J. Opt. Soc. Am.* 1986; **3**: 379.
- Dovgalenko GE, Koltz M, Salamo GJ, Wood GL. *Appl. Phys. Lett.* 1996; **68**: 287.
- Hernandez FE, Yang S, Hagan DJ, Van Stryland EW. *Mol. Cryst. Liq. Cryst.* In press.
- (a) Kost A, Tutt LW, Kelvin MB, Dougherty TK, Elias WE. *Opt. Lett.* 1993; **18**: 334; (b) Ma B, Riggs JE, Sun YP. *J. Phys. Chem.* 1998; **B102**: 5999; (c) Riggs JE, Sun YP. *J. Phys. Chem.* 1999; **A103**: 485 and references therein.
- (a) Blau W, Byrne H, Dennis WH, Kelly JM. *Opt. Commun.* 1985; **56**: 25; (b) Guha S, Kong K, Porter P, Roach JF, Remy DE, Aranda FJ, Rao DVGLN. *Opt. Lett.* 1992; **17**: 264; (c) Si J, Yang M, Wang Y, Zhang L, Li C, Wang D, Dong S, Sun W. *Appl. Phys. Lett.* 1994; **64**: 3083.
- (a) Shirk JS, Pong RGS, Bartoli FJ, Snow AW. *Appl. Phys. Lett.* 1993; **63**: 1880; (b) Perry JW, Mansour K, Marder SR, Perry KJ, Alvarez Jr. D, Choong I. *Opt. Lett.* 1994; **19**: 625; (c) Wei TH, Hagan DJ, Sence MJ, Vanstryland EW, Perry JW, Coulter DR. *Appl. Phys.* 1992; **B54**: 46; (d) Li C, Zhang L, Yang M, Wang H, Wang Y. *Phys. Rev.* 1994; **A49**: 1149; (e) Perry JW, Mansour K, Lee IYS, Wu XL, Bedworth PV, Chen CT, Ng D, Marder SR, Miles P, Wada T, Tran M, Sasabe H. *Science* 1996; **273**: 1533.
- (a) Low MKM, Hou H, Zheng H, Wong W, Jin G, Xin X, Ji W. *Chem. Commun.* 1998; 505; (b) Ji W, Du J, Tang SH, Shi S. *J. Opt. Soc. Am.* 1995; **12**: 876 and references therein.
- Perry JW, Khundar LR, Coulter DR, Alvarez Jr. D, Marder SR, Wei TH, Sence MJ, Van Stryland EW, Hagan DJ, Messier J et al. (eds). *Nato ASI Series* 1991; **E194**: 369.
- Przhonska OV, Lim JH, Hagan DJ, Stryland EWV, Bondar MV, Solminsky YL. *J. Opt. Soc. Am.* 1992; **B15**: 802.
- (a) Mansour K, Soileau MJ, Stryland EWV. *J. Opt. Soc. Am.* 1992; **B9**: 1100; (b) Joudrier V, Bourdon P, Hache F, Flytzanis C. *Appl. Phys.* 1998; **B67**: 627.
- Hochbaum A, Ferguson JL, Buck JD. *SPIE*, 1992; **1692**: 96.
- Dovgalenko GE, Klotz M, Salamo GJ, Wood GL. *Appl. Phys. Lett.* 1996; **68**: 287.
- Scalora M, Dowling JP, Bowden CM, Blemer MJ. *Phys. Rev. Lett.* 1994; **73**: 1368.
- Fischer GL, Boyd RW, Moore TR, Sipe JE. *Opt. Lett.* 1996; **21**: 1643.
- Sahyun MRV, Hill SE, Serpone N, Danesh R, Sharma DK. *J. Appl. Phys.* 1996; **79**: 8030.
- Tian JG, Zhang C, Zhang G, Li J. *Appl. Opt.* 1993; **32**: 6628.
- (a) Tutt LW, Bogges TF. *Prog. Quant. Electr.* 1993; **17**: 299; (b) Sutherland RL. *Handbook of Nonlinear Optics*. Marcel Dekker: New York, 1996; Chap. 9; (c) Nalwa HS, Miyate S. *Nonlinear Optics of Organic Molecules and Polymers*. CRC Press: Boca Raton, FL, 1997.
- Xia T, Hagan DJ, Dogariu A, Said AA, Stryland EWV. *Appl. Opt.* 1997; **36**: 4110 and references therein.
- Hollins RC. *Curr. Opin. Solid State Mater. Sci.* 1999; **4**: 189.
- Spangler CW. *J. Mater. Chem.* 1999; **9**: 2013.
- Hernandez FE, Yang S, Van Stryland EW, Hagan DJ. *Opt. Lett.* 2000; **25**: 1180.
- Rao DN, Rao SV, Blanco E, Aranda FJ, Rao DVGLN, Akkara JA. *J. Sci. Ind. Res.* 1998; **57**: 664.
- (a) Sevan A, Ravikanth M, Kumar GR. *Chem. Phys. Lett.* 1996; **263**: 241; (b) Mishra SR, Rawat HS, Laghate M. *Opt. Commun.* 1998; **147**: 328; (c) Chen P, Tomov IV, Dvornikov AS, Nakashima M, Roach JF, Alabran DM, Rentzepis PM. *J. Phys. Chem.* 1996; **100**: 17 507; (d) Su W, Cooper TM, Brant MC. *Chem. Mater.* 1998; **10**: 1212.
- (a) Wood GL, Miller MJ, Mott AG. *Opt. Lett.* 1995; **20**: 973; (b) Qureshi FM, Martin SJ, Long X, Bradley DDC, Henari FZ, Blau WJ, Smith EC, Wang CH, Kar AK, Anderson HL. *Chem. Phys.* 1998; **231**: 87; (c) Dou K, Sun X, Wang X, Parkhill R, Guo Y, Knobbe ET. *Solid State Commun.* 1998; **107**: 101.
- Rao SV, Rao DN, Akkara JA, DeCristofano BS, Rao DVGLN. *Chem. Phys. Lett.* 1998; **297**: 491.
- Rao DVGLN, Aranda FJ, Roach JF, Remy DE. *Appl. Phys. Lett.* 1991; **58**: 1241.
- Rao SV, Srinivas NKNM, Giribabu L, Maiya BG, Philip R, Kumar GR, Rao DN. *Opt. Commun.* In press.
- Henari FZ, Blau WJ, Milgrom LR, Yahioğlu G, Phillips D, Lacey JA. *Chem. Phys. Lett.* 1997; **267**: 229.
- Boyd RW. *Nonlinear Optics*. Academic Press: San Diego, 1992.
- Swatton SNR, Welford KR, Till SJ, Sambles JR. *Appl. Phys. Lett.* 1995; **66**: 1868.
- Tai-Hei W, Huang T-H, Lin H-D, Lin S-H. *Appl. Phys. Lett.* 1995; **67**: 2266.
- Dou K, Sun X, Wang X, Parkhill R, Guo Y, Knobbe ET. *IEEE J. Quantum Electron.* 1999; **35**: 1004.